

# Revisiting Flat bands and localization

Yasuhiro Hatsugai

*Department of Physics, University of Tsukuba, 1-1-1 Tennodai, Tsukuba, Ibaraki 305-8571, JAPAN*

---

## Abstract

Flat bands imply lack of itinerancy due to some constraints that, in principle, results in anomalous behaviors with randomness. By a molecular orbital (MO) representation of the flat band systems, random MO models are introduced where the degeneracy due to the flat bands is preserved even with randomness. The zero modes of the chiral symmetric system with sublattice imbalance belong to the class. After explaining the generic flat band construction by MOs, several examples are discussed with numerical demonstration as sawtooth lattice in one dimension and hyper-Pyrochlore lattice in any  $d$ -dimensions that extends the Kagome ( $d = 2$ ) and Pyrochlore ( $d = 3$ ) lattices to general dimensions.

*Keywords:* Flat bands, molecular orbitals, Kagome, Pyrochlore, randomness

---

## 1. Introduction

Massless Dirac fermions with singular dispersion are sources of non-trivial topology and get focused substantially in relation to topological phases and Anderson localization as well. Flat bands are another singular dispersion and have a long history of studies. Any projection operator of an eigen state in momentum space has degenerate eigen values (0 and 1), that gives a trivial example of the flat band. However, constructing a tight-binding Hamiltonian with strictly short range hopping is not trivial. A tight-binding Hamiltonian of a simplified  $sp^3$  network of an amorphous solid is one of the oldest examples of the flat band systems[1]. The origin of the flat bands in the model was clarified based on the molecular orbital (MO) construction[2] and the MO representation is applied to the simplified model of silicene as a two-dimensional analogue[3]. The systems with flat bands also appeared occasionally in various studies from quite different points of view such as fermion doubling[4], ferromagnetism[5, 6, 7] and ferrimagnetism[8]. The flat band is also observed experimentally in frustrated Kagome metal[9]. The flat bands of local Hamiltonian are due to some local constraints, which imply possible non trivial behaviors in Anderson localization such as multifractality[10, 11]. One of the well known origin of the flat bands is imbalance of the sublattices in a chiral symmetric system. Appearance of localized boundary modes of graphene near the Zigzag edges belong also to the class. A hopping Hamiltonian on the Penrose tiling is also in this class since the Penrose tiling is bipartite and there exist sublattices imbalance[12]. Although the system is aperiodic, the Hamiltonian hosts macroscopic degeneracy (ring states) due to the constraint. This is an example of "flat band" without translational symmetry.

Recently we are proposing a general scheme to construct a strictly local Hamiltonian with flat bands [2, 3, 13, 14]. It includes the above chiral symmetric sublattice imbalance

*Preprint submitted to Annals of Physics*

*January 6, 2022*

case. The construction is independent of the translational symmetry and can be applied to random systems. We are here introducing such a class of systems as a random MO model and present some of numerical results as a demonstration. As for the numerical evaluation of the probability density  $p_i$  and its correlation function  $C_{ij}$ , we do not need diagonalization. Also the numerical studies can be done using a sparse matrix technique since the MO is local. It enables us to treat large systems.

## 2. Molecular Orbital representation

Let us first define  $M$  molecular orbitals (MOs)  $|i\rangle$ , ( $i = 1, \dots, M$ ) as

$$|i\rangle = \sum_{n=1}^N |n\rangle \psi_{n,i} = |\mathcal{A}\rangle \psi_i, \quad |\mathcal{A}\rangle = (|1\rangle, \dots, |N\rangle),$$

where  $\psi_i$  is an  $N$ -dimensional column vector of the  $i$ -th molecular orbital and  $|\mathcal{A}\rangle$  is a set of orthonormalized atomic basis,  $\langle n|m\rangle = \delta_{nm}$ ,  $\langle \mathcal{A}|\mathcal{A}\rangle = I_N$  ( $N$  is the number of atoms).

A Hamiltonian written by the  $M$  molecular orbitals (MOs) is [2, 3, 13, 14]

$$\begin{aligned} \mathcal{H} &= \sum_{i,j}^M |i\rangle h_{i,j} \langle j| = |\mathcal{M}\rangle h \langle \mathcal{M}| = |\mathcal{A}\rangle H \langle \mathcal{A}| \\ H &= \Psi h \Psi^\dagger, \end{aligned}$$

where  $H \in M(N, N)$ ,  $h \in M(M, M)$ <sup>1</sup> and  $h_{i,j} = \{h\}_{i,j}$ , is a hopping between the molecular orbitals  $|i\rangle$  and  $|j\rangle$ . Here  $|\mathcal{M}\rangle$  is a set of the MOs' basis

$$|\mathcal{M}\rangle = (|1\rangle, \dots, |M\rangle) = |\mathcal{A}\rangle \Psi, \quad \Psi = (\psi_1, \dots, \psi_M) \in M(N, M).$$

We assume that  $\det h \neq 0$  and the MOs  $\psi_i$ ,  $i = 1, \dots, M$  are linearly independent ( $\text{rank } \Psi = M$ )<sup>2</sup>. It implies the overlap matrix  $\mathcal{O} = \langle \mathcal{M}|\mathcal{M}\rangle = \Psi^\dagger \Psi$  is positive definite ( $\det \mathcal{O} \neq 0$ ).

If  $N > M$ , this Hamiltonian  $\mathcal{H}$  has at least  $N - M$  degenerate zero modes since the zero energy condition,  $\langle \mathcal{M}|\varphi\rangle = 0$  for  $|\varphi\rangle = |\mathcal{A}\rangle \varphi$ , gives  $M$  linear conditions for  $N$ -dimensional vector  $\varphi$ .<sup>3 4 5</sup> This is true even when  $\Psi$  is random, which we propose as a random molecular orbital model[2, 17, 18].

By using an orthonormalized basis of the MOs,

$$|\bar{\mathcal{M}}\rangle = |\mathcal{M}\rangle \mathcal{O}^{-1/2}, \quad \langle \bar{\mathcal{M}}|\bar{\mathcal{M}}\rangle = I_M,$$

<sup>1</sup> $M(n, m)$  is a set of  $n \times m$  matrices.

<sup>2</sup>If  $\det h = 0$ , one can reduce the independent MOs.

<sup>3</sup>It also obeys from a simple algebra for the secular equation  $\det_N(\lambda I_N - H) = \det_N(\lambda I_N - \Psi h \Psi^\dagger) = \lambda^{N-M} \det_M(\lambda I_M - h \mathcal{O})$  [2, 13, 14].

<sup>4</sup>When the system is periodic, there exists flat bands. One may also consider  $H$  as a Hamiltonian in momentum representation and the label  $n$  as an index of the atomic species within the unit cell in momentum space. Then the zero energy flat band is  $N - M$  fold degenerated.

<sup>5</sup>This MO construction of the zero mode flat bands reminds us of the Maxwell relations for stability/instability of mechanical systems[15, 16].

the projection to the non-zero energy states,  $\mathcal{P}_1$  is written as

$$\mathcal{P}_1 = |\bar{\mathcal{M}}\rangle\langle\bar{\mathcal{M}}| = |\mathcal{A}\rangle\Psi\mathcal{O}^{-1}\Psi^\dagger\langle\mathcal{A}|.$$

Now we have an orthogonal decomposition of the one-particle Hilbert space as

$$1 = \mathcal{P}_0 + \mathcal{P}_1, \quad \mathcal{P}_i\mathcal{P}_j = \delta_{ij}\mathcal{P}_i,$$

where  $\mathcal{P}_1$  and  $\mathcal{P}_0$  are projections to the non-zero/zero energy states respectively ( $\mathcal{H}\mathcal{P}_1 = \mathcal{H}$  and  $\mathcal{H}\mathcal{P}_0 = 0$ ). Then the complementary projection to the zero modes is written as

$$\begin{aligned} \mathcal{P}_0 &= 1 - \mathcal{P}_1 = |Z\rangle\langle Z|, \quad \langle Z|Z\rangle = I_{N-M} \\ |Z\rangle &= (|\varphi_1\rangle, \dots, |\varphi_{N-M}\rangle), \quad \langle M|\varphi_i\rangle = 0 \\ |\varphi_\ell\rangle &= |\mathcal{A}\rangle\varphi_\ell, \quad H\varphi_\ell = 0, \end{aligned}$$

where  $|\varphi_\ell\rangle$ ,  $\ell = 1, \dots, N-M$  are orthonormalized states of the zero mode,  $\langle\varphi_\ell|\varphi_{\ell'}\rangle = \delta_{\ell\ell'}$ .

To discuss properties of localization of the wave function  $\varphi_\ell$  of the zero energy, the probability distribution  $p_i^\ell = C_{ii}^\ell = |\varphi_{i,\ell}|^2$  and the correlation function  $C_{ij}^\ell = \varphi_{i,\ell}\varphi_{j,\ell}^*$  can be useful. However, the exact degeneracy of the flat band implies that each  $\varphi_\ell$  is not uniquely defined and one may take another set of the zero energy states,  $|Z'\rangle = (|\varphi'_1\rangle, \dots, |\varphi'_{N-M}\rangle)$ . Of course  $|Z\rangle$  and  $|Z'\rangle$  are unitary equivalent as  $|Z'\rangle = |Z\rangle U$ ,  $U \in U(N-M)$ . Then what is invariant (independent of the transformation  $U$ ) is an average or a trace over the degenerate states defined as

$$\begin{aligned} C_{ij} &= \sum_{\ell=1}^{N-M} C_{ij}^\ell = \sum_{\ell=1}^{N-M} \varphi_{i,\ell}\varphi_{j,\ell}^* = \langle i|\mathcal{P}_0|j\rangle = \delta_{ij} - \tilde{C}_{ij} \\ \tilde{C}_{ij} &= (\Psi\mathcal{O}^{-1}\Psi^\dagger)_{ij}. \end{aligned}$$

Its invariance is clear by  $\mathcal{P}_0 = |Z\rangle\langle Z| = |Z'\rangle\langle Z'|$ . The local probability of the site  $i$  for the zero mode space defined as  $p_i = C_{ii}/M$ , ( $\sum_i p_i = 1$ ) is the average of the local probability distribution of  $p_i^\ell$ . This is the only well-defined quantity that is independent of the choice of the states. One may wonder effects of the randomness might be washed out by the average. However it is not the case as shown in the concrete examples discussed in the next section. Since the projection into the zero energy space  $\mathcal{P}_0$  is independent of the hopping between the MOs,  $h_{ij}$ , we assume  $h = I_M$  without loss of generality as far as the degenerate zero energy space is concerned.

Note also that  $C_{ij}$  is also written as a correlation function of the filled zero modes  $|z\rangle_F$  of the second quantized fermions as

$$\begin{aligned} C_{ij} &= {}_F\langle z|c_j^\dagger c_i|z\rangle_F \\ |z\rangle_F &= \prod_{\ell=1}^{N-M} \mathbf{c}^\dagger \varphi_\ell |0\rangle_F, \end{aligned}$$

since  ${}_F\langle z|c_i c_j^\dagger|z\rangle_F = \delta_{ij} - \langle i|\mathcal{P}_0|j\rangle$  where  $c_i$ , ( $i = 1, \dots, N$ ) is a fermion annihilation operator ( $\{c_i, c_j^\dagger\} = \delta_{ij}$ ),  $\mathbf{c}^\dagger = (c_1, \dots, c_N)$  and  $|0\rangle_F$  is their vacuum ( $c_i|0\rangle_F = 0$ ). See appendix A.

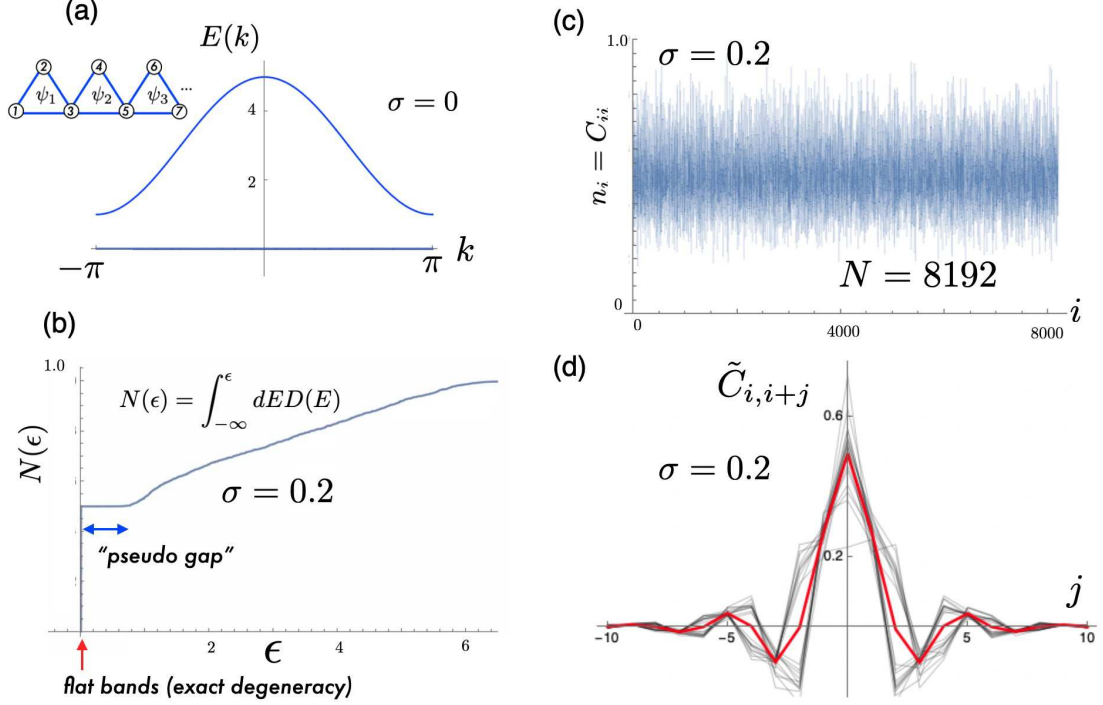


Figure 1: (a): Sawtooth lattice and its energy dispersion for  $a = b = c = 1$ . (b) Integrated density of states  $N(\epsilon)$  ( $\sigma = 0.2$ ) (c) "Charge"  $n_i = C_{ii}$  of the zero energy space ( $N = 2M = 8192$ ) with periodic boundary condition. Normalized probability density  $p_i = n_i/M$ . (d) "Correlation function"  $\tilde{C}_{i,i+j}$  of the zero energy space. The black lines are for 21 different  $i$ 's and the red one is their average.

### 3. Examples

#### 3.1. Sawtooth lattice in 1D

The simplest example with a flat band is a one-dimensional sawtooth lattice ( Fig.1(a)) This model has been discussed in many papers (See.[19], for example). The Hamiltonian is written by  $M$ -MO,  $|j\rangle = |\xi_j\rangle\xi_j^1 + |\eta_j\rangle\eta_j + |\xi_{j+1}\rangle\xi_j^2$ , ( $j = 1, \dots, M$ ) for an  $N = 2M$  site system as  $H = \sum_{j=1}^M |j\rangle\langle j|$  where  $|\xi_j\rangle$  and  $|\eta_j\rangle$  are orthonormalized atomic states and  $\xi_j^1, \xi_j^2, \eta_j \in \mathbb{C}$  are arbitrary. We assume periodic boundary condition  $|\xi_{M+1}\rangle = |\xi_1\rangle$  for simplicity. Since the Hamiltonian is written by  $M$  MOs and the number of the atomic sites is  $N = 2M$ , it has  $N - M = M$  degenerate zero energy states. If the system is translational invariant as  $\xi_j^1 = a, \xi_j^2 = b, \eta_j = c$ , one has  $H = \sum_{k_n} |k_n\rangle\langle k_n|$ ,  $|k_n\rangle = (|\xi_{k_n}\rangle, |\eta_{k_n}\rangle)\psi_{k_n}$ ,  ${}^t\psi_{k_n} = (a + ce^{ik_n}, b)$  in the momentum representation  $|\xi_j\rangle = M^{-1/2} \sum_{k_n} |\xi_{k_n}\rangle e^{ik_n j}$ ,  $|\eta_j\rangle = M^{-1/2} \sum_{k_n} |\eta_{k_n}\rangle e^{ik_n j}$ ,  $k_n = \frac{2\pi n}{M}, n = 1, \dots, M$ . Now its non-zero energy band is given by  $\psi_{k_n}^\dagger \psi_{k_n} = |a + be^{ik_n}|^2 + |c|^2$  and the rest is the flat band at the zero energy.

We have calculated probability distribution  $p_i$  and its correlation function  $C_{ij}$  for the random MO sawtooth model in Fig.1(b)-(d). The random MOs are defined by  $\xi_i^{1,2} = 1 + X_i^{1,2}$  and  $\eta_i = 1 + X_j$  where  $X_i^{1,2}$  and  $X_i$  are random variables of the normal

distribution with variance  $\sigma^2$  and its mean 0. In the Fig.1(b), the integrated density of states is shown for  $\sigma = 0.2$ . The charge  $n_i$  is shown for  $\sigma = 0.2$  for  $N = 8192$  system in Fig.1. It is very spiky and behaves randomly in a microscopic scale. We have also calculated inverse participation ratios (IPR),  $I = \sum_i p_i^4$ , ( $p_i = n_i/M$ ,  $\sum_i p_i = 1$ ) for different system sizes ( $N = 8$  to  $N = 8192$ ). It behaves  $\mathcal{O}(1/N)$  that suggests the space is extended since it is an average of the IPR of the degenerated zero energy states. Also the correlation function  $\tilde{C}_{i,i+j}$  is plotted in Fig.1(d) averaged over several  $i$ 's. It suggests the average  $\tilde{C}_{ij}$  is exponentially localized, that is, the zero energy space is short-ranged and its localization length is roughly several lattice spacing. It implies that the zero mode space is intrinsically localized due to the local nature of the MO within microscopic space and the macroscopic degeneracy makes the whole zero mode space extended as is shown in the IPR.

### 3.2. Hyper-Pyrochlore lattice in $d$ -dimensions

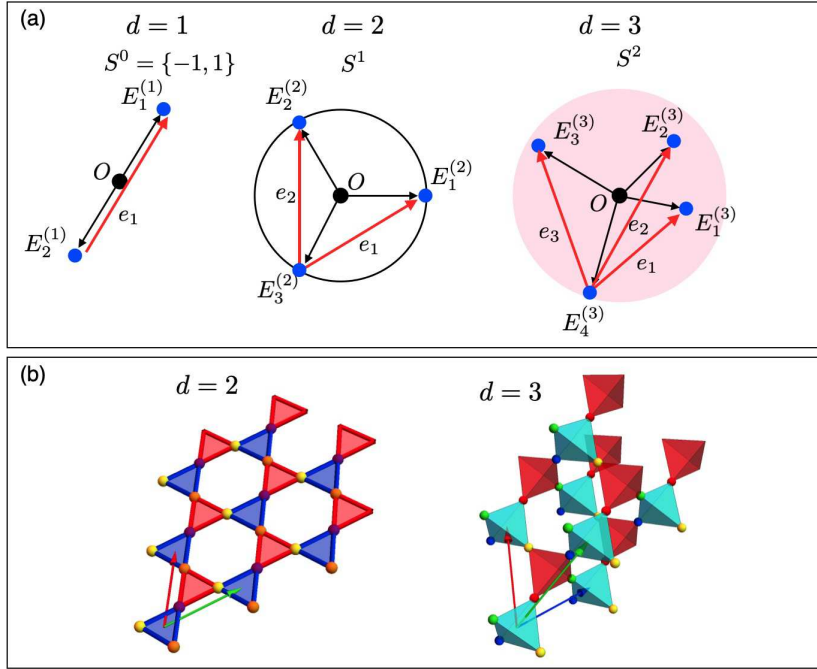


Figure 2: (a) Unit vectors  $e_i$ ,  $j = 1, \dots, d$  for a series of hyper-Pyrochlore lattices[2]. Equivalent  $(d+1)$  points  $E_j^{(d)}$ ,  $j = 1, \dots, d+1$  are distributed on the Sphere  $S^{d-1}$ . (b) Several lattice points and its unit vectors are shown for  $d = 2$  (Kagome) and  $d = 3$  (Pyrochlore).

We have also proposed a series of systems with flat bands in  $d$ -dimensions as a hyper-Pyrochlore lattice[2]. This is dual to the  $d$ -dimensional graphene that is an extension of 4- $d$  graphene[20]. Energy bands of the hyper-Pyrochlore are given by the (shifted) bands of  $d$ -dimensional graphene with extra  $(d-1)$ -fold degenerated flat bands at zero energy[2]. As the  $d$ -dimensional graphene is a minimum model for the massive/massless

Dirac fermions in  $d$ -dimension, the hyper-Pyrochlore lattice is also minimum as a system with flat bands in general dimension.

Let us start from  $(d-1)$ -dimensional sphere  $S^{d-1}$  (See Fig.2(a)) and  $d+1$  points,  $E_1^{(d)}, \dots, E_{d+1}^{(d)}$  which are equivalently distributed on the unit sphere ( $E_j^{(d)} \cdot E_{j'}^{(d)} = -d^{-1}$ ,  $j = 1, \dots, d+1$ ).<sup>6</sup> Then the unit translations,  $e_1, \dots, e_d$ , are given by  $e_j = e_j^{(d)} = E_j^{(d)} - E_{d+1}^{(d)}$ . The unit cell of the hyper-Pyrochlore lattice includes  $d+1$  atoms which locate at  $-e_1/2, \dots, -e_{d+1}/2$ , ( $e_{d+1} = 0$  is supplemented).

With periodic boundary condition of the linear size  $L$ ,  $(d+1)L^d$  atomic positions of the system with  $L^d$  unit cells are

$$r_j = r - e_j/2, \quad (j = 1, \dots, d+1),$$

where  $r = n_1 e_1 + \dots + n_d e_d$  and  $n_j = 1, \dots, L$ , ( $j = 1, \dots, d$ ). See Fig.2(b). The Hamiltonian of the hyper-Pyrochlore is written as

$$H = \sum_r (|B_r\rangle\langle B_r| + |R_r\rangle\langle R_r|).$$

Two MOs,  $|B_r\rangle$  and  $|R_r\rangle$  at the unit cell  $r$  are defined as

$$\begin{aligned} |B_r\rangle &= \sum_{j=1}^{d+1} |r_j\rangle \xi_r^j \\ |R_r\rangle &= \sum_{j=1}^{d+1} |r + e_j\rangle \eta_r^j, \end{aligned}$$

where  $|r_j\rangle$  and  $|r + e_j\rangle$  are orthonormalized atomic states at the sites. The weights (coefficients) within the MO,  $\xi_r^j, \eta_r^j \in \mathbb{C}$ , can be any. As for the numerical demonstration, we take  $\xi_r^j = 1 + X_r^j$  and  $\eta_r^j = 1 + Y_r^j$  where  $X_r^j$  and  $Y_r^j$  are random variables of the normal distribution with variance  $\sigma^2$  and its means 0. Since the number of the atomic sites is  $N = (d+1)L^d$  and that of the MOs is  $M = 2L^d$ , the system has  $N - M = (d-1)L^d$  zero energies. If the system is translationally invariant, that is,  $\xi_r^j$  and  $\eta_r^j$  are  $r$ -independent, the system has (at least)  $(d-1)$ -fold degenerate flat bands (at the zero energy). In a translationally invariant clean system, the Hamiltonian in momentum space is written by the MOs in momentum space. Then the flat band is give by the momentum independent zero mode(see footnote in page 2). In this case, the MOs are momentum dependent and may not be always linearly independent. If the MOs are not independent,  $\det \mathcal{O} = 0$ , it causes extra degeneracies such as band touching[21, 2, 13].

Numerical results for the case  $d = 2$ , that is, the random MO Kagome lattice is shown in Fig.3. They are comparable to the results of the one-dimensional sawtooth lattice. In

---

<sup>6</sup>They are recursively constructed from  $d = 1$  by

$$E_j^{(d)} = \begin{cases} \alpha_d E_j^{(d-1)} + \beta_d E_{d+1}^{(d)} & j = 1 \dots, d \\ {}^t(0, \dots, 0, 1_d, 0, \dots) & j = d+1 \end{cases},$$

where  $\alpha_d = \sqrt{1 - d^{-2}}$  and  $\beta_d = -d^{-1}$ . Here we have assumed the system is embedded in sufficiently large dimension.

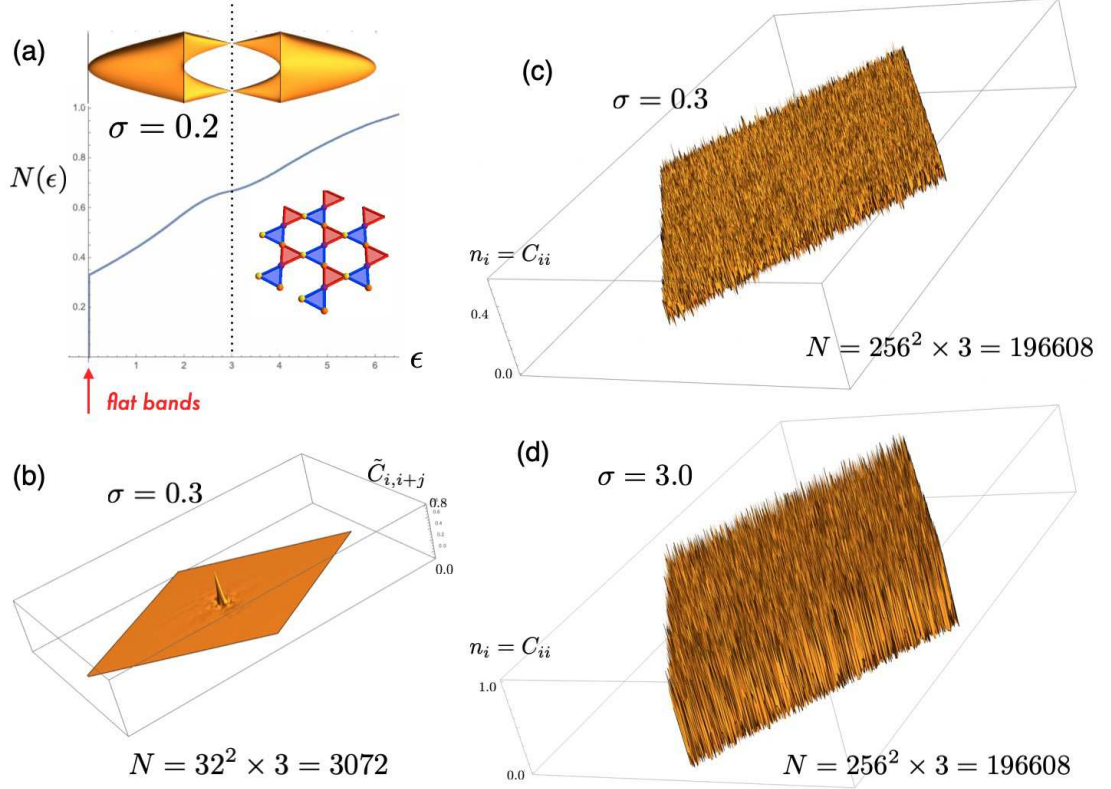


Figure 3: (a) Integrated density of states for Kagome lattice without randomness ( $\xi_r^j = \eta_r^j = 1$ ). (b) "Correlation function"  $\tilde{C}_{i,i+j}$  of the zero energy space ( $N = 3 \times 32^2$ ). (c) "Charge"  $n_i = C_{ii}$  of the zero energy space ( $N = 3M = 3 \times 256^2$ ) with periodic boundary condition. Normalized probability density  $p_i = n_i/M$ . ( $\sigma = 0.3$ ) (d) "Charge"  $n_i = C_{ii}$  of the zero energy space ( $N = 3M = 3 \times 256^2$ ) with periodic boundary condition. Normalized probability density  $p_i = n_i/M$ . ( $\sigma = 3.0$ )

Fig.3(a), the integrated density of states for the random MO Kagome model is shown ( $\sigma = 0.2$ ). The Dirac cones for the clean case is also shown for reference. The "correlation function"  $\tilde{C}_{i,i+j}$  of the zero energy space is shown in Fig.3(b) for a rather small system ( $N = 3 \times 32^2$ )  $i$  is at the center of the system. It also shows the correlation function is short-ranged over several lattice spacing. Charge distributions/probability distribution  $n_i$  are shown in Fig.3(c),(d) for  $\sigma = 0.3$  and  $\sigma = 3.0$  respectively ( $N = 3 \times 256^2$ ). They show the distribution is very spiky over several to 10 lattice spacing. We have also calculated IPR,  $I = \sum_i p_i^4$ , ( $p_i = n_i/M$ ,  $\sum_i p_i = 1$ ) for  $N = 3 \times L^2$ ,  $L = 2^4$  to  $2^7$ . This is the average of the IPR's over the degenerate zero energy states this is unitary invariant. They behave  $\mathcal{O}(1/L^2)$  that is consistent with the extended states. It suggests the zero mode space is microscopically quite spiky but extended globally. It is similar to the results of the one-dimensional sawtooth lattice.<sup>7</sup> Similarly to the results of the

<sup>7</sup>When one uses the method in Ref.[22] for calculating a singularity spectrum (multifractal analysis),

sawtooth lattice, the zero mode space of the random MO Kagome lattice is intrinsically short-ranged (this is also true without any randomness). It is consistent with the spiky behavior of the probability distribution within a microscopic scale. However, due to the macroscopic degeneracy, the space as a whole is extended as shown by the IPR.

At the mobility edge of the Anderson localization as the critical point, one may naturally expect multifractal behaviors of the wave function since the localization length diverges and the system is scale free. Away from the critical point, such a multifractal behavior is cut off at the localization length. It implies that the wave function of localized states is multifractal-like up to the localization length. Even for the present Kagome flat band system, one may expect standard Anderson localization except the flat bands. As discussed, the zero mode flat band space, that is, the average of the flat bands are complementary to the sum of them those are localized and their localization centers are randomly chosen. The spiky structure observed in  $C_{ij}$  is reflecting this multifractal-like behavior within the localization length.

### 3.3. Bipartite lattice

If the lattice sites are divided into two sublattices A and B and the hopping matrix elements are only non-zero between them, the lattice is bipartite and the corresponding Hamiltonian written in the atomic basis is chiral symmetric. By the choice of the MO in Ref.[13], it is written by the MOs as

$$\begin{aligned}\mathcal{H}_C &= \sum_{a \in A, b \in B} (|a\rangle_A t_{ab} \langle b| + |b\rangle_B t_{ab}^* \langle a|) \\ &= |\mathcal{A}\rangle D_{AB} \langle \mathcal{B}| + |\mathcal{B}\rangle D_{BA} \langle \mathcal{A}| \\ &= |\mathcal{A}, \mathcal{B}\rangle H_C \langle \mathcal{A}, \mathcal{B}| \\ H_C &= \begin{pmatrix} O_{AA} & D_{AB} \\ D_{BA} & O_{BB} \end{pmatrix} \\ |\mathcal{A}, \mathcal{B}\rangle &= (|\mathcal{A}\rangle, |\mathcal{B}\rangle), \quad |\mathcal{A}\rangle = (|1\rangle_A, \dots, |N_A\rangle_A), \quad |\mathcal{B}\rangle = (|1\rangle_B, \dots, |N_B\rangle_B),\end{aligned}$$

where  $D_{BA} = D_{AB}^\dagger \in M(N_A, N_B)$ ,  $\{D_{AB}\}_{ab} = t_{ab}$  and  $H_C$  is chiral symmetric  $\{H_C, \Gamma\} = 0$  with  $\Gamma = \text{diag}(I_A, -I_B)$ . It is also written by  $M = 2N_B$  MOs,  $\Psi$  as [13]<sup>8</sup>

$$\begin{aligned}\mathcal{H}_C &= |\mathcal{M}\rangle h \langle \mathcal{M}|, \quad |\mathcal{M}\rangle = (|\mathcal{A}\rangle D_{AB}, |\mathcal{B}\rangle) = |\mathcal{A}, \mathcal{B}\rangle \Psi \\ \Psi &= \begin{pmatrix} D_{AB} & O_{AB} \\ O_{BB} & I_{N_B} \end{pmatrix} \in M(N_A + N_B, 2N_B), \\ h &= \begin{pmatrix} O_{BB} & I_{N_B} \\ I_{N_B} & O_{BB} \end{pmatrix} \in M(2N_B, 2N_B).\end{aligned}$$

Since the number of total atomic sites is  $N = N_A + N_B$ , the Hamiltonian has  $Z = N - M = N_A - N_B$  zero modes if  $N_A > N_B$ . (The case,  $N_B > N_A$ , is discussed similarly.)

---

after averaging over a box of the size  $\ell$ , taking an extrapolation  $\ell \rightarrow 0$  is needed. Using the average over the box size  $\ell$  up to several lattice spacing, numerical multifractal analysis of the wave functions of the random MO Kagome lattice has been performed by exact diagonalizations[18]. It suggests multifractality of the flat band wave functions in a microscopic scale (over several lattice spacing). To obtain conclusive results, further analysis is needed.

<sup>8</sup> $O_{\alpha\beta} \in M(N_\alpha, N_\beta)$  is a zero matrix ( $\alpha, \beta \in \{A, B\}$ ).

It implies that the chiral symmetric (random) system is regarded as the (random) MO model. One of the historical examples of the flat band due to this mechanism is the ring states of the Penrose tiling[12] and discussed from a generic point of view[23]. Another typical example is the zero energy state of the random Dirac fermions[24], where  $N_A - N_B = 1$  and the zero mode wave function is discussed in relation to its multifractality.

#### 4. Discussion

As has been discussed previously[10, 11], the states near the flat band energy become singular by randomness and their multifractality has been implied. In the random MO models presented in examples of the sections 2 and 3, macroscopic degeneracy of the flat bands is preserved even with randomness. This macroscopic degeneracy makes the situation unclear although the zero mode space obtained numerically is very local and singular in a microscopic scale. It is also consistent with the numerical calculation in Ref.[24] where the zero mode is not degenerated ( $Z = N - M = 1$ ). Then introducing extra MOs associated with the randomness can be interesting. If one introduces macroscopic  $M'$  extra random MOs ( $M + M' \lesssim N$ ), the dimension of the zero energy space can be  $\mathcal{O}(1)$ . Also the MO representation are useful for diagonalization of random systems within the projected flat band subspace.

#### 5. Acknowledgment

We thank discussion with T. Mizoguchi and T. Kuroda. This work is supported in part by the JSPS KAKENHI, Grant No. JP17H06138.

#### Appendix A. Fermion correlation function

Let us here discuss fermion correlation functions for a filled fermi state. We label the Fock state  $|\Psi\rangle_F$  specified by the multiplet,  $\Psi \in M(N, M)$ , of the dimension  $M$  for the dimension  $N$  Hilbert space as

$$|\Psi\rangle_F = \prod_{\ell=1}^M (c^\dagger \psi_\ell) |0\rangle_F = (c^\dagger \psi_1) \cdots (c^\dagger \psi_M) |0\rangle_F = \prod_{\ell=1}^M (c_j^\dagger \psi_\ell^j) |0\rangle_F$$

$$\Psi = (\psi_1, \cdots, \psi_M), \quad \psi_\ell = \begin{pmatrix} \psi_{1,\ell} \\ \vdots \\ \psi_{N,\ell} \end{pmatrix}, \quad c = \begin{pmatrix} c_1 \\ \vdots \\ c_N \end{pmatrix},$$

where  $|0\rangle_F$  a vacuum,  $c_i |0\rangle_F = 0$ , and the ordering of the fermions are implicitly assumed as shown above. The overlap of such two fermionic states  $|\Phi\rangle_F$  and  $|\Psi\rangle_F$  is directly evaluated as

$${}_F\langle\Psi|\Phi\rangle_F = \det_M \Psi^\dagger \Phi.$$

Using this, the correlation function,  $g_{ab}^U = {}_F\langle\Psi|c_a c_b^\dagger|\Phi\rangle_F$ , is written as

$$g_{ab}^U = {}_F\langle\Psi|c_a c_b^\dagger|\Phi\rangle_F = \det_{M+1} \Psi_a^\dagger \Phi_b$$

where  $\Phi_a = (e_a, \Phi) \in M(N, M+1)$ ,  $\Psi_b = (e_b, \Psi) \in M(N, M+1)$  are obtained from  $\Phi$  and  $\Psi$  by adding column vectors  $e_a$  and  $e_b$  respectively where  $\{e_i\}_j = \delta_{ij}$ .

Using a formula for the determinant<sup>9</sup>, it is calculated as

$$\begin{aligned}
g_{ab}^U &= \det_{M+1} \begin{pmatrix} e_a^\dagger \\ \Psi^\dagger \end{pmatrix} (e_b, \Phi) = \det_{M+1} \begin{pmatrix} e_a^\dagger e_b & e_a^\dagger \Phi \\ \Psi^\dagger e_b & \Psi^\dagger \Phi \end{pmatrix} \\
&= \det_{M+1} \begin{pmatrix} e_a^\dagger e_b - e_a^\dagger \Phi (\Psi^\dagger \Phi)^{-1} \Psi^\dagger e_b & 0 \\ \Psi^\dagger e_b & \Psi^\dagger \Phi \end{pmatrix} \\
&= \det_1 [e_a^\dagger e_b - e_a^\dagger \Phi (\Psi^\dagger \Phi)^{-1} \Psi^\dagger e_b] \det_M (\Psi^\dagger \Phi) \\
&= \det_1 [e_a^\dagger [I_N - \Phi (\Psi^\dagger \Phi)^{-1} \Psi^\dagger] e_b] \det_M (\Psi^\dagger \Phi) \\
&= [I_N - \Phi (\Psi^\dagger \Phi)^{-1} \Psi^\dagger]_{ab} \det_M (\Psi^\dagger \Phi).
\end{aligned}$$

It implies

$$\begin{aligned}
g_{ab} &\equiv \frac{F \langle \Psi | c_a c_b^\dagger | \Phi \rangle_F}{F \langle \Psi | \Phi \rangle_F} = g_{ab}^U / \det_M (\Psi^\dagger \Phi) = [g]_{ab} \\
g &= I_N - \Phi (\Psi^\dagger \Phi)^{-1} \Psi^\dagger \\
\tilde{g}_{ba} &= \frac{F \langle \Psi | c_b^\dagger c_a | \Phi \rangle_F}{F \langle \Psi | \Phi \rangle_F} = [\Phi (\Psi^\dagger \Phi)^{-1} \Psi^\dagger]_{ab}
\end{aligned}$$

Similarly the 4-point correlation function is evaluated as

$$\begin{aligned}
g_{ba;cd}^U &= F \langle \Psi | c_b c_a c_c^\dagger c_d^\dagger | \Phi \rangle_F \\
&= \det_{M+2} \begin{pmatrix} e_{ab}^\dagger \\ \Psi^\dagger \end{pmatrix} (e_{cd}, \Phi), \quad e_{ab} = (e_a, e_b), \quad e_{cd} = (e_c, e_d) \\
&= \det_2 [e_{ab}^\dagger e_{cd} - e_{ab}^\dagger \Phi (\Psi^\dagger \Phi)^{-1} \Psi^\dagger e_{cd}] \det_M (\Psi^\dagger \Phi) \\
&= \det_2 [e_{ab}^\dagger [I_N - \Phi (\Psi^\dagger \Phi)^{-1} \Psi^\dagger] e_{cd}] \det_M (\Psi^\dagger \Phi) \\
&= \det_2 \left[ \begin{pmatrix} e_a^\dagger \\ e_b^\dagger \end{pmatrix} [I_N - \Phi (\Psi^\dagger \Phi)^{-1} \Psi^\dagger] \begin{pmatrix} e_c \\ e_d \end{pmatrix} \right] \det_M (\Psi^\dagger \Phi)
\end{aligned}$$

It implies the Wick theorem

$$\begin{aligned}
g_{ba;cd} &\equiv \frac{F \langle \Psi | c_b c_a c_c^\dagger c_d^\dagger | \Phi \rangle_F}{F \langle \Psi | \Phi \rangle_F} = g_{ba;cd}^U / \det_M (\Psi | \Phi) \\
&= \det_2 \begin{pmatrix} e_a^\dagger \\ e_b^\dagger \end{pmatrix} g(e_c, e_d) \\
&= g_{ac} g_{bd} - g_{ad} g_{bc}.
\end{aligned}$$

<sup>9</sup>As for  $A \in M(N, N)$ ,  $B \in M(N, M)$ ,  $C \in M(M, N)$ ,  $D \in M(M, M)$  and  $\det_M D \neq 0$ , the following relation holds,

$$\begin{aligned}
\det_{N+M} \begin{pmatrix} A & B \\ C & D \end{pmatrix} &= \det_{N+M} \begin{pmatrix} I_N & -BD^{-1} \\ O_{MN} & I_M \end{pmatrix} \begin{pmatrix} A & B \\ C & D \end{pmatrix} = \det_{N+M} \begin{pmatrix} A - BD^{-1}C & O_{NM} \\ C & D \end{pmatrix} \\
&= \det_N (A - BD^{-1}C) \det_M D
\end{aligned}$$

A generic case for the  $2M$ -point function follows straightforwardly as

$$\begin{aligned}
g_{a_M \cdots a_2 a_1; b_1 b_2 \cdots b_M} &\equiv \frac{F \langle \Psi | c_{a_M} \cdots c_{a_1} c_{b_1}^\dagger \cdots c_{b_M}^\dagger | \Phi \rangle_F}{F \langle \Psi | \Phi \rangle_F} \\
&= \det_M e_{a_1, \dots, a_M}^\dagger g_{b_1, \dots, b_M} \\
&= \det_M g^R,
\end{aligned}$$

where  $e_{i_1, \dots, i_M} = (e_{i_1}, \dots, e_{i_M}) \in M(N, M)$  and  $\{g^R\}_{i,j} = g_{a_i b_j}$ , ( $i, j = 1, \dots, M$ ).

## References

- [1] D. Weaire, M. F. Thorpe, Electronic properties of an amorphous solid. i. a simple tight-binding theory, *Phys. Rev. B* 4 (1971) 2508–2520. doi:10.1103/PhysRevB.4.2508.  
URL <https://link.aps.org/doi/10.1103/PhysRevB.4.2508>
- [2] Y. Hatsugai, I. Maruyama,  $Z_Q$  topological invariants for polyacetylene, kagome and pyrochlore lattices, *EPL (Europhysics Letters)* 95 (2) (2011).
- [3] Y. Hatsugai, K. Shiraishi, H. Aoki, Flat bands in the weaire–thorpe model and silicene, *New Journal of Physics* 17 (2) (2015).
- [4] E. Dagotto, E. Fradkin, A. Moreo, A comment on the nielsen-ninomiya theorem, *Physics Letters B* 172 (3) (1986) 383 – 386. doi:[https://doi.org/10.1016/0370-2693\(86\)90274-1](https://doi.org/10.1016/0370-2693(86)90274-1).  
URL <http://www.sciencedirect.com/science/article/pii/0370269386902741>
- [5] A. Mielke, Ferromagnetic ground states for the hubbard model on line graphs, *Journal of Physics A: Mathematical and General* 24 (2) (1991) L73–L77. doi:10.1088/0305-4470/24/2/005.  
URL <https://doi.org/10.1088/0305-4470/24/2/005>
- [6] H. Tasaki, Ferromagnetism in the hubbard models with degenerate single-electron ground states, *Phys. Rev. Lett.* 69 (1992) 1608–1611. doi:10.1103/PhysRevLett.69.1608.  
URL <https://link.aps.org/doi/10.1103/PhysRevLett.69.1608>
- [7] H. Katsura, I. Maruyama, A. Tanaka, H. Tasaki, Ferromagnetism in the hubbard model with topological/non-topological flat bands, *EPL (Europhysics Letters)* 91 (5) (2010) 57007. doi:10.1209/0295-5075/91/57007.  
URL <https://doi.org/10.1209/0295-5075/91/57007>
- [8] E. H. Lieb, Two theorems on the hubbard model, *Phys. Rev. Lett.* 62 (1989) 1201–1204. doi:10.1103/PhysRevLett.62.1201.  
URL <https://link.aps.org/doi/10.1103/PhysRevLett.62.1201>
- [9] M. Kang, S. Fang, L. Ye, H. C. Po, J. Denlinger, C. Jozwiak, A. Bostwick, E. Rotenberg, E. Kaxiras, J. G. Checkelsky, R. Comin, Topological flat bands in frustrated kagome lattice cosn, *Nature Communications* 11 (1) (2020) 4004. doi:10.1038/s41467-020-17465-1.  
URL <https://doi.org/10.1038/s41467-020-17465-1>
- [10] M. Goda, S. Nishino, H. Matsuda, Inverse anderson transition caused by flatbands, *Phys. Rev. Lett.* 96 (2006) 126401. doi:10.1103/PhysRevLett.96.126401.  
URL <https://link.aps.org/doi/10.1103/PhysRevLett.96.126401>
- [11] J. T. Chalker, T. S. Pickles, P. Shukla, Anderson localization in tight-binding models with flat bands, *Phys. Rev. B* 82 (2010) 104209. doi:10.1103/PhysRevB.82.104209.  
URL <https://link.aps.org/doi/10.1103/PhysRevB.82.104209>
- [12] M. Kohmoto, B. Sutherland, Electronic states on a penrose lattice, *Phys. Rev. Lett.* 56 (1986) 2740–2743.
- [13] T. Mizoguchi, Y. Hatsugai, Molecular-orbital representation of generic flat-band models, *EPL (Europhysics Letters)*.
- [14] T. Mizoguchi, Y. Hatsugai, Systematic construction of topological flat-band models by molecular-orbital representation, *Physical Review B* 101 (23) (2020).
- [15] J. Maxwell, L. on the calculation of the equilibrium and stiffness of frames, *Phil. Mag.* 27 (1864) 294–299.
- [16] J. Paulose, B. G.-g. Chen, V. Vitelli, Topological modes bound to dislocations in mechanical metamaterials, *Nature Physics* 11 (2) (2015) 153–156. doi:10.1038/nphys3185.  
URL <https://doi.org/10.1038/nphys3185>
- [17] Y. Hatsugai, K. Kohda, unpublished.

- [18] K. Kohda, Master thesis, University of Tsukuba (2017) (Japanese).
- [19] Y. Kuno, T. Mizoguchi, Y. Hatsugai, Flat band quantum scar, *Phys. Rev. B* 102 (2020) 241115. doi:10.1103/PhysRevB.102.241115. URL <https://link.aps.org/doi/10.1103/PhysRevB.102.241115>
- [20] M. Creutz, Four-dimensional graphene and chiral fermions, *Journal of High Energy Physics* 2008 (04) (2008) 017–017. doi:10.1088/1126-6708/2008/04/017. URL <https://doi.org/10.1088/1126-6708/2008/04/017>
- [21] D. L. Bergman, C. Wu, L. Balents, Band touching from real-space topology in frustrated hopping models, *Phys. Rev. B* 78 (2008) 125104. doi:10.1103/PhysRevB.78.125104. URL <https://link.aps.org/doi/10.1103/PhysRevB.78.125104>
- [22] A. Chhabra, R. V. Jensen, Direct determination of the  $f(\alpha)$  singularity spectrum, *Phys. Rev. Lett.* 62 (1989) 1327–1330. doi:10.1103/PhysRevLett.62.1327. URL <https://link.aps.org/doi/10.1103/PhysRevLett.62.1327>
- [23] B. Sutherland, Localization of electronic wave functions due to local topology, *Phys. Rev. B* 34 (1986) 5208–5211. doi:10.1103/PhysRevB.34.5208. URL <https://link.aps.org/doi/10.1103/PhysRevB.34.5208>
- [24] Y. Hatsugai, X.-G. Wen, M. Kohmoto, Disordered critical wave functions in random-bond models in two dimensions: Random-lattice fermions at  $\nu=0$  without doubling, *Physical Review B* 56 (3) (1997) 1061–1064.